International Journal of Current Engineering and Technology
E-ISSN 2277 – 4106, P-ISSN 2347 – 5161

Available at http://inpressco.com/category/ijcet

Research Article

Thermodynamic Analysis and Multi-Objective Optimizations of a Combined Recompression SCO_2 Brayton Cycle-TCO_2 Rankine Cycles for Waste Heat Recovery

Ali S. Alsagri[#*] and Andrew D. Chiasson[^]

[#]Qassim University, Unizah, Qassim, Saudi Arabia
^University of Dayton, Dayton, OH, USA

Received 05 March 2018, Accepted 08 May 2018, Available online 12 May 2018, **Vol.8, No.3 (May/June 2018)**

Abstract

A thermodynamic analysis and optimization of a newly-conceived combined power cycle were conducted in this paper for the purpose of improving overall thermal efficiency of power cycles by attempting to minimize thermodynamic irreversibilities and waste heat as a consequence of the Second Law. The power cycle concept comprises a topping advanced recompression supercritical carbon dioxide (sCO2) Brayton cycle and a bottoming transcritical carbon dioxide (tCO2) Rankine cycle. The bottoming cycle configurations included a simple tCO2 Rankine cycle and a split tCO2 Rankine cycle. The topping sCO2 recompression Brayton cycle used a combustion chamber as a heat source, and waste heat from a topping cycle was recovered by the tCO2 Rankine cycle due to an added high efficiency recuperator for generating electricity. The combined cycle configurations were thermodynamically modeled and optimized using an Engineering Equation Solver (EES) software. Simple bottoming tCO2 Rankine cycle cannot fully recover the waste heat due to the high exhaust temperature from the top cycle, and therefore an advance split tCO2 Rankine cycle was employed in order to recover most of the waste heat. Results show that the highest thermal efficiency was obtained with recompression sCO2 Brayton cycle – split flow tCO2 Rankine cycle. Also, the results show that the combined CO2 cycles is a promising technology compared to conventional cycles.

Keywords: *Rankine cycle, Brayton cycle, sCO2, tCO2, Engineering Equation Solver etc.*

Introduction

The unprecedented growth in the world population and economic activity, along with rising concerns about environmental issues, mean that energy efficiency will play a vital role in the development of future energy systems. Motivated by limited energy resources, the accelerating growth of energy demand, cost, and growing environmental concerns, there has been a focus on improving such poor energy production efficiency.

Recently, CO_2 as a working fluid is a well-known source that has been a technology of interest (O. P. Sharma *et al*, 2017; M. Marchionni *et al*, 2018; J. Song *et al*, 2018; A. A. Gkountas, *et al*, 2017; C. W. White *et al*, 2017; S. Kim *et al*. 2018; X. Wang *et al*, 2017). Researchers have demonstrated that low exhuast temperature can power supercritical and transcritical CO_2 Rankine cycles (M. T. Dunham *et al*, 2013; J. Sarkar *et al*, 2015; J. F. Hinze *et al*, 2017; Y. Cao, 2016,2017).

*Corresponding author **Ali S. Alsagri** (ORCID ID: 0000-0002-0142-7386) is working as Assistant Professor and **Andrew D. Chiasson** as Professor, DOI: https://doi.org/10.14741/ijcet/v.8.3.9

Sarker provides an organized review of tCO_2 Rankine cycle configurations from the literature, focusing on low-grade heat supplies, and he provides a performance comparison with other working fluids. He finds that the tCO_2 Rankine cycle has clear advantages to steam and organic Rankine cycles (ORC), and he discusses pathways to developing aspects of this cycle (parameter optimization, hardware components, control strategies, etc.). Wang and Dai compared the exergoeconomic performance for two bottoming cycles (tCO_2 and ORC) designed to optimize waste heat recovery from a sCO_2 recompression Brayton topping cycle. Parametric optimization indicates that the tCO_2 bottoming cycle has superior performance at lower pressure ratio (PRc) (off-design conditions), and that higher turbine inlet temperatures improve tCO2 exergoeconomic performance, unlike the ORC. Both combined cycles have similar second-law efficiency, and the ORC was shown to have a slightly lower total product unit cost. Yari and Sirousazar developed a tCO_2 cycle for recovering waste heat from the pre-cooler of a sCO_2 Brayton cycle, and they modeled the performance improvement for this new combined cycle relative to that of a simple sCO_2 cycle. The authors reported that their new system improved the first and second law efficiencies by 5.5%, to 26%, and that it reduced exergy destruction by 6.7%, to 28.8%. Chen et. al. compared the performance of two cycles act as a bottoming cycle to extract useful work from low-grade waste heat. The ORC is most commonly used, but the authors found that the tCO_2 power cycle showed better performance. Specifically, this cycle had a slightly higher power output than ORC, and it did not have a pinch limitation in the heat exchanger.

Table 1 Literature input parameters and combined power cycle efficiency

-	Wang		Akbari	Yari	Wang	Besarati	Pichel
Top cycle	sCO_2	sCO_2	sCO_2	sCO_2	sCO_2	sCO_2	sCO_2
Bottom cycle	tCO_2	ORC Isopentane	ORC Isopentane	ORC Isopentane	tCO_2	ORC (R245ca)	ORC (R134a)
Main compressor inlet temperature [°C]	32		35	35	32	55	30
Main compressor inlet pressure [MPa]	7.4		7.4	7.4	8	-	7.4
Maximum pressure [MPa]	20.72		22.2	24.3386	20	25	25
Turbine inlet temperature [°C]	550		550	650	550	800	500
HTR effectiveness [-]	86%		86%	86%	95%	95%	95%
LTR effectiveness [-]	86%		86%	86%	95%	95%	95%
Turbine efficiency [%]	90/70		90/87	90/80	90/85	90/87	93/85
Compressor/Pump efficiency [%]	85/80		85/80	85/80	89/85	89/85	89/80
Pressure drop [-]	negligible		negligible	negligible	negligible	negligible	50 kPA/HX
Combined Cycle efficiency	0.449	0.4523	0.4422	0.49	0.4672	0.5433	0.435

According to the literature that shown in Table 1, most research in sCO_2 cycles used two ways to represent heat exchanger performance: using fixed heat exchanger effectiveness or pinch point temperature differences. However, due to CO_2 properties, assuming a constant recuperator effectiveness - minimum-temperature approach leads to markedly different conductance values in heat exchanger size and consequently cost. The first contribution in this study is developing a computationally efficient technique to design heat exchangers by using constant conductance (UA) to represent heat exchanger performance and thereby deliver improved accuracy in calculations. The second contribution in this research is the newly-conceived combined power cycle is proposed.

Nomenclature

sCO_2	Supercritical Carbon Dioxide
tCO_2	Transcritical Carbon Dioxide
ORC	Organic Rankine Cycle
HTF	Heat Transfer Fluid
PR	Pressure Ratio
EES	Engineering Equation Solver
UA	Heat Exchanger Conductance
Cp	Specific Heat
HTR	High Temperature Recuperator
LTR	Low Temperature Recuperator
LMTD	Log-Mean Temperature Difference
PCHE	Printer Circuit Heat Exchangers
TIT	Turbine Inlet Temperature
CIT	Compressor Inlet Temperature
WHR	Waste Heat Recovery
GA	Genetic Algorithm

Mathematical Modeling Approach

Carbon dioxide (CO_2) properties sharply vary at and near critical points (T=30.98 °C & P=7.38 MPa). illustrates the instability of CO_2's specific heat (Cp) (the amount of thermal energy needed to raise the temperature of a system by 1 °C per unit of mass) near the critical point, presenting a variety of temperatures and pressures. Despite the sCO_2 advantages of reducing the compressor work due to high density near critical points, the thermodynamic characteristics fluctuate wildly, thereby influencing the CO_2 properties. The sharp alteration in pressure and temperature near critical point makes specific heat an impractical measure. As CO_2 properties fluctuate near the critical point, design difficulties with turbomachinery and heat exchangers arise [20]. So, following the conventional method that assume a constant capacity to deal with a heat exchanger whose properties change arbitrarily near the critical point is invalid (K. Gregory *et al*, 2009). An adjustment needs to be made in order to reuse the convectional equations, which are described in detail in the heat exchanger model in the next section.

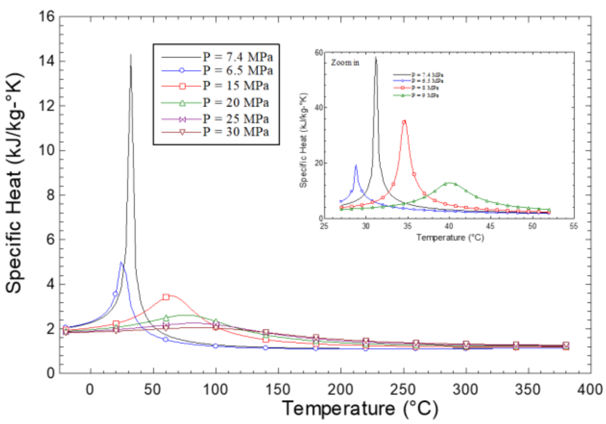

Figure 1 Specific heat variation at different temperatures and pressures

In this study, two combined CO_2 power cycles are subjected to thermodynamic analysis and optimization in order to improve calculation accuracy and to improve the cycle efficiency and power output. With respect to improving the accuracy of the analytical model, a computationally efficient technique using constant conductance (UA) to represent heat exchanger performances is executed. The cycles involved will be 1) a top sCO_2 recompression Brayton cycle with a bottom tCO_2 split flow Rankine cycle -called cycle I- (Figure.2a) and 2) a top sCO_2 recompression Brayton cycle with a bottom tCO_2 simple Rankine cycle –called cycle II- (figyre.2b).

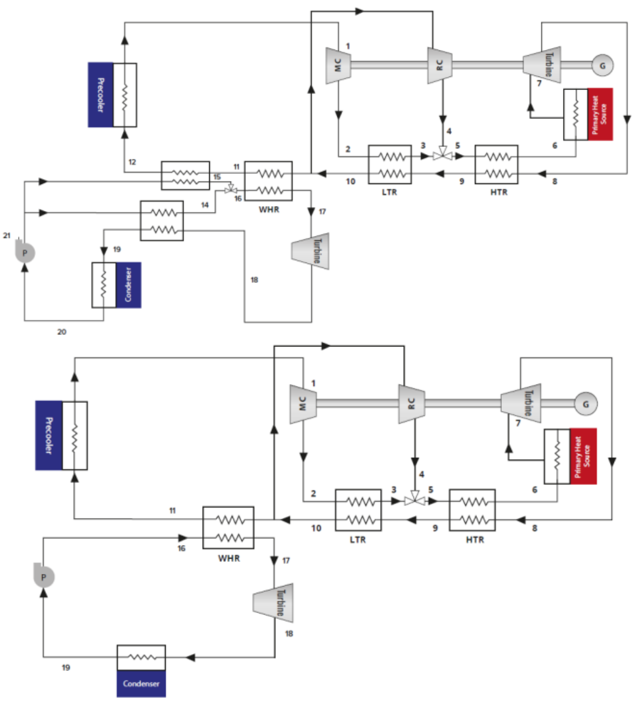

Figure 1 Combined CO2 power cycles a) recompression sCO2 Bryton cycle – split flow tCO2 Rankine cycle b) recompression sCO2 Bryton cycle – simple tCO2 Rankine cycle

Turbomachinery

Turbomachinery analysis is modeled on the energy balance (energy conservation) of each components to study the performance of turbines, compressors, and the pump. In this research, the focus is on the off-design performance of the turbomachinery components. For turbomachinery modeling, some basic assumptions are considered: (i) the cycle functions in a steady state; (ii) the turbine expansion, compressors, and pump are adiabatic with given isentropic efficiencies; (iii) the effect of kinetic and potential energy are negligible; (iv) each component of the cycle is sufficiently insulated. The compressors (η_c) and turbine (η_t) isentropic efficiencies are defined as:

$$\eta_c = \frac{h_{out}-h_{in}}{h_{out_{ise}}-h_{in}} \quad (1)$$

$$\eta_t = \frac{h_{in}-h_{out}}{h_{in}-h_{out_{ise}}} \quad (2)$$

where h_{in} and h_{out} are the actual inlet and outlet enthalpies, respectively, and $h_{out_{ise}}$ is the isentropic outlet enthalpy. Two properties at any state are sufficient to calculate the others properties in the same state. The inlet turbine and compressor temperature and pressure are assumed, while taking into consideration the pressure drop in the cycle. With known two-inlet turbomachinery properties and one-outlet turbomachinery properties, the model obtains the turbomachinery outlet properties using equations (3) and (4):

$$s_{in} = s_{out_{ise}} \quad (3)$$

$$h_{out_{ise}} = f\ (P_{out}\ ,\ s_{out_{ise}}) \quad (4)$$

Where s_{in} and $s_{out_{ise}}$ are the inlet actual specific entropy and outlet isotropic specific entropy respectively. After specific isentropic outlet enthalpy is calculated in equation the actual enthalpy can be obtained using the isentropic turbomachinery efficiencies.

The specific actual work can be calculated using equation (5)

$$w = h_{in} - h_{out} \quad (5)$$

Heat exchanger

The conventional techniques for the analysis of heat exchangers (log-mean temperature difference (LMTD) and effectiveness-NTU) rely upon assumptions to set up the equations, such as constant specific heat. These techniques are not valid for recuperators operating under inconstant capacitances, such as CO_2 near the critical point. To overcome this impediment, two approaches will be explored: Develop a numerical complex model or divide the heat exchanger into numerous small sub heat exchangers (Nodalization).

In the model presented below, the printed-circuit heat exchangers (PCHEs) are divided into sub-heat exchangers (nodalization) as it is shown in figure 3. Nodalization is a heat exchanger modeling strategy that is necessary when a CO_2 working fluid is used due to its significant properties changing at or near the critical point. Each sub heat exchanger is then modeled independently (each component is evaluated as a separate control volume). At each sub-heat exchanger, the capacitance is almost the same and therefore the conventional techniques (LMTD and effectiveness-NTU) can be used after the adjusting of heat exchanger.

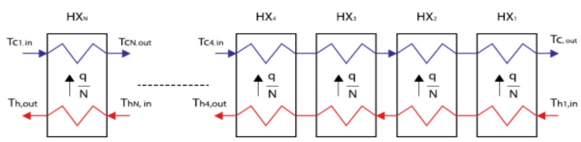

Figure 3 Sub-heat exchangers

The appropriate number of sub-heat exchangers were studied to characterize the high variation of properties near the critical point. Too many nodes slow down the computational analysis, while too few nodes reduce the calculation accuracy. The system is first modeled with 20 sub-heat exchangers for each heat exchanger in the cycle, then dropped to 15, where there was not a big difference in the system efficiency. Then it reduces to 10 sub-heat exchangers, the efficiency still looks identical. Then, when the system is modeled with 8 sub-heat exchangers, a slight difference occurs. Finally, the system is tested with 6 sub-heat exchangers, there is a noticeable difference.

Figure 2 Figure 2 shows different number of sub-heat exchangers versus cycle efficiency. Starting with ten sub-heat exchangers, the efficiency starts to converge. From 10 to 20 nodes, the efficiency seems identical, and therefore, 10 sub-heat exchangers seem to be enough for analysis.

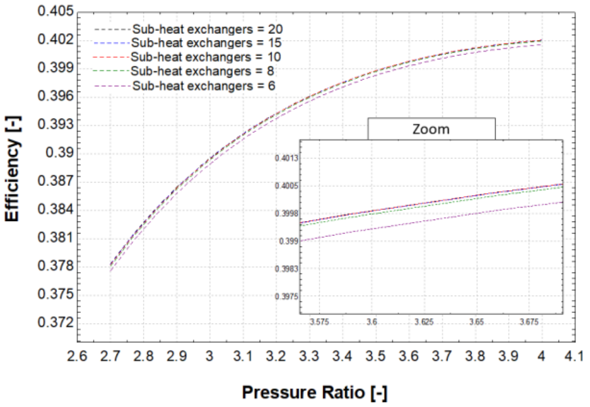

Figure 2 Efficiency at different number of Sub-Heat Exchangers

The counter-flow effectiveness and number of transfer units (NTU) is shown in equations (6) and (7) respectively.

$$\varepsilon = \frac{1-\exp[-NTU*(1-C_R)]}{1-C_R*\exp[-NTU*(1-C_R)]} \quad (6)$$

$$NTU = \frac{\ln[\frac{1-C_R}{1-\varepsilon}]}{1-C_R} \quad (7)$$

Where C_R represents the dimensionless capacity ratio describing the heat exchanger balanced.

With the nodalization method, the total heat transfer rate is calculated first in either one of equations (8) and (9) using an energy balance, then it is equally divided between the sub-heat exchangers by using equation (10) and (11)

$$\dot{q_H} = \dot{C}_H * (T_{h_{in}} - T_{h_{out}}) = \dot{m}_H * (h_{h_{in}} - h_{h_{out}}) \quad (8)$$

$$\dot{q_C} = \dot{C}_C * (T_{C_{in}} - T_{C_{out}}) = \dot{m}_C * (h_{C_{in}} - h_{C_{out}}) \quad (9)$$

$$\dot{q_H} = \dot{q_C} \quad (10)$$

$$q_i = \frac{\dot{q}_{total}}{N} \quad (11)$$

Where $\dot{C}_H$, $\dot{C}_C$ and $\dot{m}_H$, $\dot{m}_C$ are the capacitance rate and mass flow rate of the hot and cold streams respectively, $T_{h_{in}}$, $T_{C_{in}}$ and $h_{h_{in}}$, $h_{C_{in}}$ are the inlet temperature and enthalpy of the hot and cold streams, $T_{H_{out}}$, $T_{C_{out}}$ and $h_{h_{out}}$, $h_{C_{out}}$ are the out temperature and enthalpy of the hot and cold streams respectively, and N is the number of sub-heat exchangers.

Then enthalpies for each sub-heat exchangers is calculated using equation (12) and (13)

$$h_{h_{out}} = h_{h_{in}} - \frac{\dot{q}_i}{\dot{m}_h} \quad (12)$$

$$h_{c_{out}} = h_{c_{in}} - \frac{\dot{q}_i}{\dot{m}_c} \quad (13)$$

Where $\dot{m}_h$ and $\dot{m}_c$ are the mass flow rate of hot and cold streams, $\dot{q}$ is the heat transfer rate of the sub-heat exchanger.

Calculation of the average specific heat C_p heat and heat capacity rate ($\dot{C}$) of each side for the sub-heat exchanger, is done through equations (14), (15) and (16)

$$C_{P_h} = \frac{(h_{h_{in}} - h_{h_{out}})}{(T_{h_{in}} - T_{h_{out}})} \quad (14)$$

$$C_{P_C} = \frac{(h_{C_{out}} - h_{C_{in}})}{(T_{C_{out}} - T_{C_{in}})} \quad (15)$$

$$C_h = \dot{m}_H * C_{P_h} \quad (16)$$

$$C_c = \dot{m}_c * C_{P_c} \quad (17)$$

To calculate the sub-heat exchanger performance, the dimensionless effectiveness (ε) is defined in equation (18)

$$\varepsilon = \frac{\dot{q}_\iota}{\dot{q}_{\iota max}} = \frac{\dot{q}_\iota}{C_{min}*(T_{h_{in}} - T_{c_{out}})} \quad (18)$$

Calculating the conductance for each sub-heat exchanger as it shown in equation (19)

$$UA_i = C_{min} * NTU_i \quad (19)$$

Where NTU is the dimensionless number of transfer units that are defined in equation (19)

Optimization

The Multi-objective optimization technique conducted in this work is based on a genetic algorithm (GA) using Engineering Equation Solver (EES). Using the GA method allows the model to handle non-linear and non-differentiable optimization tasks. The two objective targets in the optimization processes are: 1) the overall thermal efficiency and 2) the power output.

Both objective targets need to be maximized simultaneously, while at some points they are conflicted to each other. Thus, the weighted sum method is employed in this study for the purpose of properly solving the conflicted of the multi-objective functions.

Optimization Domain

For an appropriate optimization, the variables bounds have to be predetermined to govern the optimization process and provide more reliable solutions. Based on the literature review at Table 1, the upper and lower bounds are specified. The lower and upper bounds set at the acceptable values to allow the model to test as mush variables as it could be. The optimization domain of the lower and upper variables is shown is the Table 2.

Table 2 Variables Lower and Upper bounds

Lower Bound	≤ Variables ≤	Upper Bound
15	Maximum pressure [MPa]	25
1	Pressure ratio	6
15	Total conductance [kW/K]	50
500	Turbine Inlet Temperature [K]	800
280	Compressor Inlet Temperature [K]	350
350	Recompressor Inlet Temperature [K]	700
1	Total mass flow rate [kg/s]	100
0	Split ratio [-]	1
0	Recompression fraction [-]	1

Design Values

As noted above, several cycle configurations will be thermodynamically modeled and optimized for thermal efficiency and power output using Engineering Equation Solver Software (EES).

Table 3 Decision and design variables

Decision variables	Cycle I	Cycle II
compressor inlet temperature (C)	32	32
compressor inlet pressure [MPa]	6.8	6.8
Pump inlet temperature	25	25
Turbine Isentropic efficiency [%]	93	93
Compressor Isentropic efficiency [%]	89	89
Inlet cooling air temperature [C]	22	22
Inlet heating air temperature [C]	900	900
Recompressor efficiency [%]	89	89
Design variables		
Main compressor inlet pressure	vary	vary
Mass Flow rate	vary	vary
Pressure Ratio	vary	vary
Total fixed UA	vary	vary
Recompression fraction [-]	vary	vary
second WHR	Vary	-
Turbine inlet temperature (C)	Vary	Vary
Compressor inlet temperature (C)	Vary	Vary

The primary heater inlet temperatures source is assumed to come from a concentrated solar power tower plant. While air-cooled heat rejection is used instead of water-cooled heat rejection to reduce water consumption. Despite the air-cooled shortcomings such as overall thermal efficiency penalty and larger air-cooled heat exchanger than wet-cooled heat exchanger, the scarce of water makes air-cooled heat rejection attractive.

The input variables are divided into two categories, decision variables and design variables. The main difference is that the decision variables are assumed to be constant for all runs, while the design variables are the optimizer which is varied for each run. The initial parameter assumptions of the heat exchangers and turbomachinery are presented in Table 3

Results and Discussion

The parametric analysis of the maximum cycle operating temperature show that the simple bottom Rankine cycle cannot fully recover the waste heat from the top recompression sCO_2 Brayton cycle. Thus, a newly-conceived bottom cycle is proposed to utilize the remaining waste heat from the top cycle. Figure 3 and Figure 4 shows thermal efficiency, exergy efficiency, and power output of the two combined cycles at different maximum operating temperature.

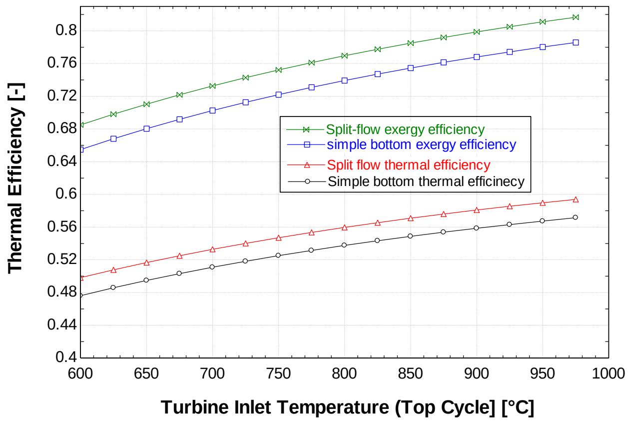

Figure 3 Thermal and Exergy efficiency comparison as a function of maximum operating temperature for the simple and new combined cycles

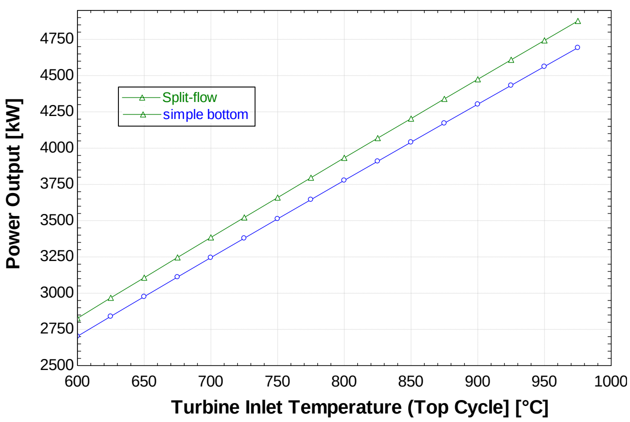

Figure 4 Power output comparison as a function of maximum operating temperature for the simple and new combined cycles

Figure 3 indicates that the energetic and exergetic efficiency increase with the increase of the maximum cycle operating temperature of both combined cycles. While increasing ambient temperature increases the external irreversibilities (exergy losses) and therefore reducing the system performance. Another interesting finding is that, exergy and energy efficiency follow the same pattern, which they are linearly increasing as the turbine inlet temperature increases. Figure 3 shows how higher energetic and exergetic of the newly-conceived cycle at all different maximum cycle operating temperatures can be achieved by adding two recuperators to unitize the remaining waste heat that the simple bottom Rankine cycle cannot recover. The newly-conceived cycle, using two more recuperators, increase the cycle efficiency by about 2% to 2.5% compared to the simple bottom cycle.

Figure 4 demonstrates the higher power output of the newly-conceived cycle compared to the simple bottom cycle when they operate at same maximum turbine inlet temperature. An interesting finding from the simple bottom tCO_2 Rankine cycle results is that, increasing the maximum operating temperature, above 390 C, leads to two conflicts results. The first result is increasing the cycle efficiency, and the second result is lowering the waste heat recovery effectiveness, and thereby having a lower system efficiency. So, system thermal efficiency is optimized by balancing the cycle efficacy against the waste heat recovery effectiveness to have a higher system efficiency. Thus, the simple bottom cycle turbine inlet temperature has to be less than 390 C in order to maintain a high waste heat recovery effectiveness. Otherwise, a drop in the waste heat recovery effectiveness occur which lower the system efficiency. To overcome this issue, a newly-conceived cycle is proposed. It allows higher bottom cycle turbine inlet temperature without adverse effecting the waste hear recovery effectiveness by adding two recuperators to the system. Increasing the maximum cycle operating temperature lead to an increase of enthalpy difference across the turbine and therefore an increase of power output.

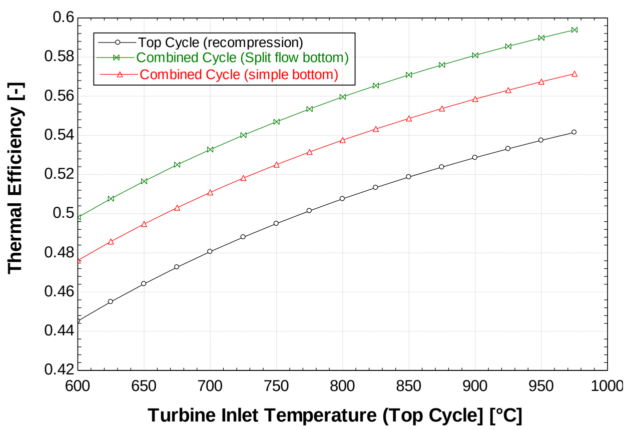

Figure 5 Thermal efficiency improvement as a function of maximum operating temperature for simple and new combined cycles

According to Figure 5 the combined cycles improve the overall cycle thermal efficiency by about 2% - 2.5% (simple bottom cycle), and 4% - 4.5% (split-flow bottom cycle) compared to the stand-alone recompression sCO2 Brayton cycle. The optimum turbine inlet temperature is determined based on the concentrated solar power (CSP) heat source availability, which will be studied in a future work. Also, economic analysis are important to be combined with the power cycle analysis to find out whether that higher efficiency, due to the higher operating temperature, is associated with the higher cost, due to larger heat exchanger and higher temperature material, worth or not.

The impact of the main compressor inlet temperature on the first law efficiency, second law efficiency, power output has been studied, as it shown in Figure 8 and Figure 9.

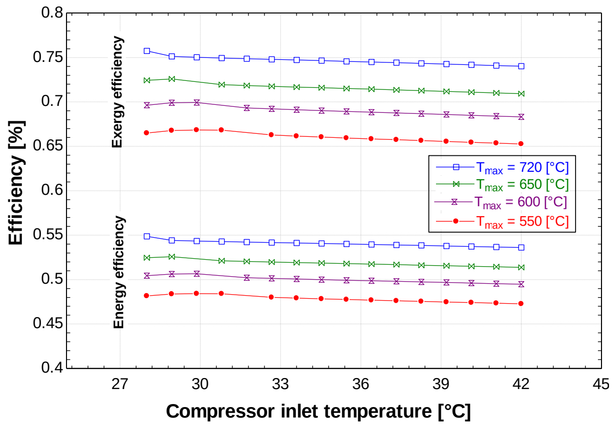

Figure 6 Impact of compressor inlet temperature and turbine inlet temperature on the newly-conceived cycle efficiency

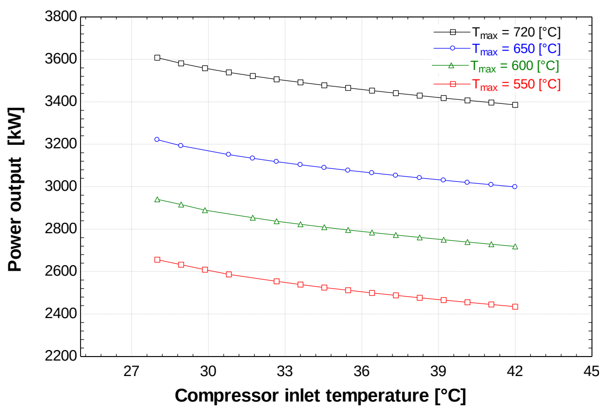

Figure 7 Impact of compressor inlet temperature and turbine inlet temperature on the newly-conceived cycle power output

Figure 8 and Figure 9 show how the minimum operating inlet temperature and maximum operating inlet temperature affect the cycle efficiency and power output. Increasing the turbine inlet temperature has a direct positive effect to the power output and efficacy. Also, it is important to note that, a high-temperatureresistant material may be needed with the increasing of maximum operating temperature, thereby increasing the system cost.

Exergy analysis of the newly-conceived combined power cycle is conducted in order to identify thermodynamic losses in each cycle component for the purpose of improving overall thermal efficiency by attempting to minimize thermodynamic irreversibilities. External irreversibilities (exergy loss) and internal irreversibilities (exergy destruction) have been determined through the exergy analysis, as they shown in Figure 8

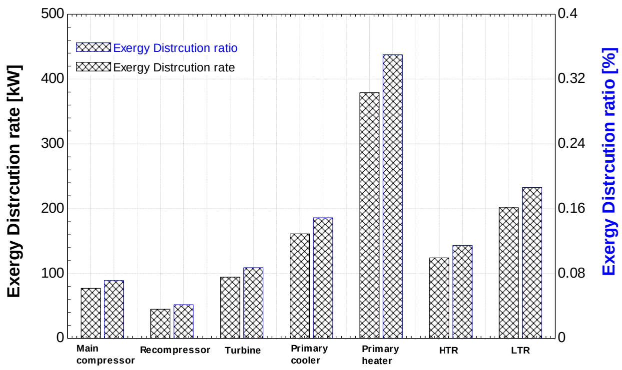

Figure 8 Exergy destructions rate and ratio in the S-CO2 components

Figure 8 shows the exergy destruction in the top recompression sCO_2 cycle components. Primary heater, which transfer heat from the primary source to the cycle, accounts for 35% of the thermodynamic losses, follow by the low temperature recuperator, which has an internal cycle heat transfer, accounts for 18% of the total thermodynamic losses. One way to minimize the thermodynamic losses on the primary heat exchanger and low temperature recuperator is to minimize heat exchanger temperature difference between the two streams (cold – hot).

Conclusion

The energy and exergy analysis of the two advanced combined cycles were conducted in this paper. The internal irreversibilities (exergy destruction) and external irreversibilities (exergy losses) for each component were investigated in order to provide appropriate guiding improvements. The top sCO_2 recompression Brayton cycle's waste heat is utilized by a bottom tCO_2 Rankine cycle for the purpose of improving both efficiency and power output. The result demonstrate that the newly-conceived cycle, sCO_2 recompression Brayton coupled with a tCO_2 split-flow Rankine cycle, surpasses the simple combined cycle, sCO_2 recompression Brayton coupled with a tCO_2 simple Rankine cycle, in respect to energy and exergy efficiencies and power output.

Based on the exergy analysis, primary heater has the highest thermodynamic losses, follow by the low temperature recuperator (LTR). On the other hand, the turbine and compressors have the lowest thermodynamic losses. The high potential improvements of the cycle should be focused on the heat exchangers and especially primary heater and low temperature recuperator.

Acknowledgments

The authors acknowledge that the work presented here was funded by Qassim University, Saudi Arabia.

O. P. Sharma, S. C. Kaushik, and K. Manjunath (2017), Thermodynamic analysis and optimization of a supercritical CO2regenerative recompression Brayton cycle coupled with a marine gas turbine for shipboard waste heat recovery, Therm. Sci. Eng. Prog., vol. 3, pp. 62–74.

M. Marchionni, G. Bianchi, and S. A. Tassou (2018), Techno-economic assessment of Joule-Brayton cycle architectures for heat to power conversion from high-grade heat sources using CO2in the supercritical state, Energy, vol. 148, pp. 1140–1152.

Song, X. Li, X. Ren, and C. Gu (2018), Performance improvement of a preheating supercritical CO 2 (S-CO 2) cycle based system for engine waste heat recovery, Energy Convers. Manag., vol. 161, no. February, pp. 225–233.

A. A. Gkountas, A. M. Stamatelos, and A. I. Kalfas (2017), Thermodynamic Modeling and Comparative Analysis of Supercritical, Proc. ASME Turbo Expo 2017 Turbomach. Tech. Conf. Expo., pp. 1–11.

C. W. White and N. T. Weiland (2017), Evaluation of Property Methods for Modeling Direct-Supercritical CO 2 Power Cycles, J. Eng. Gas Turbines Power, vol. 140, no. 1, p. 11701.

S. Kim, Y. Cho, M. S. Kim, and M. Kim (2018), Characteristics and optimization of supercritical CO2recompression power cycle and the influence of pinch point temperature difference of recuperators, Energy, vol. 147, pp. 1216–1226.

X. Wang, Q. Liu, Z. Bai, J. Lei, and H. Jin (2017), Thermodynamic Analysis of the Cascaded Supercritical CO2 Cycle Integrated with Solar and Biomass Energy, Energy Procedia, vol. 105, pp. 445–452.

M. T. Dunham and W. Lipiński (2013), Thermodynamic Analyses of Single Brayton and Combined Brayton–Rankine Cycles for Distributed Solar Thermal Power Generation, J. Sol. Energy Eng., vol. 135, no. 3, p. 31008.

J. Sarkar (2015), Review and future trends of supercritical CO2 Rankine cycle for low-grade heat conversion., Renew. Sustain. Energy Rev., vol. 48, pp. 434–451.

J. F. Hinze, G. F. Nellis, and M. H. Anderson (2017), Cost comparison of printed circuit heat exchanger to low cost periodic flow regenerator for use as recuperator in a s-CO2 Brayton cycle, Appl. Energy, vol. 208, no. August, pp. 1150–1161.

Y. Cao, J. Ren, Y. Sang, and Y. Dai (2017), Thermodynamic analysis and optimization of a gas turbine and cascade CO2combined cycle, Energy Convers. Manag., vol. 144, pp. 193–204.

Y. Cao, Y. Gao, Y. Zheng, and Y. Dai (2016), Optimum design and thermodynamic analysis of a gas turbine and ORC combined cycle with recuperators, Energy Convers. Manag., vol. 116, pp. 32–41.

X. Wang and Y. Dai (2016), Exergoeconomic analysis of utilizing the transcritical CO2cycle and the ORC for a recompression supercritical CO2cycle waste heat recovery: A comparative study, Appl. Energy, vol. 170, pp. 193–207.

M. Yari, M., & Sirousazar (2010), A novel recompression S-CO2 Brayton cycle with pre-cooler exergy utilization, Proc. Inst. Mech. Eng. Part A J. Power Energy, vol. 224, no. 7, pp. 931–946.

Y. Chen, P. Lundqvist, A. Johansson, and P. Platell (2006), A comparative study of the carbon dioxide transcritical power cycle compared with an organic rankine cycle with R123 as working fluid in waste heat recovery, Appl. Therm. Eng., vol. 26, no. 17–18, pp. 2142–2147.

S. M. S. S. M. S. Mahmoudi, A. R. Ghavimi, X. Wang, Y. Dai, A. D. Akbari, and S. M. S. S. M. S. Mahmoudi (2016), Thermoeconomic analysis & optimization of the combined supercritical CO2 (carbon dioxide) recompression Brayton/organic Rankine cycle, Energy, vol. 170, pp. 501–512.

Y. Wang, X., Wang, J., Zhao, P., & Dai (2015), Thermodynamic comparison and optimization of supercritical CO 2 Brayton cycles with a bottoming transcritical CO 2 cycle, J. Energy Eng., vol. 142, no. 3.

S. M. Besarati (2014), Analysis of Advanced Supercritical Carbon Dioxide Power Cycles for Concentrated Solar Power Applications, Univ. South Florida.

G. D. Pérez-pichel, J. I. Linares, L. E. Herranz, B. Y. Moratilla, and R. Mari (2012), Thermal analysis of supercritical CO 2 power cycles : Assessment of their suitability to the forthcoming sodium fast reactors, Nucl. Eng. Des., vol. 250, pp. 23–34.

V. Dostal (2004), A Supercritical Carbon Dioxide Cycle,.

K. Gregory, Nellis (2009); Sanford, Heat Transfer, 1st ed. cambridge university press.